In situ monitoring of the photorefractive response time in a self-adaptive wavefront holography setup developed for acousto-optic imaging

Max Lesaffre, F. Jean, François Ramaz, Albert-Claude Boccara, Michel Gross, Philippe Delaye, Gérald Roosen

In situ monitoring of the photorefractive response time in a self-adaptive wavefront holography setup developed for acousto-optic imaging

M. Lesaffre, F. Jean, F. Ramaz, A.C. Boccara

Laboratoire d'Optique, Ecole Supérieure de Physique et de Chimie Industrielles de la Ville de Paris, CNRS UPRA0005, Université Pierre et Marie Curie, 10 rue Vauquelin F-75231 Paris cedex 05

ramaz@optique.espci.fr

M. Gross

Laboratoire Kastler-Brossel, UMR 8552 (ENS, CNRS, UMPC), Ecole Normale Supérieure, 10 rue Lhomond F-75231 Paris cedex 05

P. Delaye, G. Roosen

Laboratoire Charles Fabry de l'Institut d'Optique, CNRS, Université Paris-Sud, Campus Polytechnique, RD128, F-91127, Palaiseau cedex

Abstract: The measurement of optical contrasts within thick biological tissues can be performed with the hybrid technique of acousto-optic imaging, but it has been shown that an acquisition rate in the $1-10kHz$ range is required for a good efficiency. This comes from the interferometric nature of the signal, blurred by speckle decorrelation in a time τ_c, due to a decrease of the speckle pattern contrast at the exit of the sample. An holographic setup that associates a fast and large area single photodetector and a photorefractive crystal, can measure in *real-time* the acousto-optic signal: this is the so-called *self-adaptive wavefront holography* technique. Nevertheless, it is essential to size the photorefractive response time (τ_{PR}) of the crystal with τ_c in order to optimize the signal-to-noise ratio of the measurement. This time mainly depends on the overall light intensity within the crystal. We have developed an original *in situ* method to determine τ_{PR} with the combination of acoustic pulses and a frequency de-tuning of the reference beam. We can measure precisely this time but also *monitor* it according to a theoretical model that we have previously described. We are able to adapt the response time of the setup to the decorrelation time of the medium under study.

OCIS codes: (170.1650) Coherence imaging; (170.3660) Light propagation in tissues; (290.7050) Turbid media; (090.0090) Holography; (090.2880) Holographic interferometry; (170.7050) Turbid media

References and links

1. A.P. Gibson, J.C. Hebden, S.R. Arridge, "Recent advances in diffuse optical imaging," Phys. Med. Biol **50**, 1-43 (2005).

#75639 - $15.00 USD Received 2 October 2006; revised 17 November 2006; accepted 27 November 2006

2. L.H. Wang, S.L. Jacques and X. Zhao, "Continuous wave ultrasonic modulation of scattered light to image objcets in turbid media," Opt. Lett. **20**, 629 (1995).
3. W. Leutz and G. Maret, "Ultrasonic modulation of multiply scattered light," Physica B **204**, 14 (1995).
4. L. Wang, "Mechanisms of ultrasonic modulation of multiply scattered coherent light: a analytic model," Phys. Rev. Lett. **87**, 1 (2001).
5. M. Kempe, M. Larionov, D. Zaslavsky, and A. Z. Genack, "Acousto-optic tomography with multiple scattered light," J. Opt. Soc. Am. B **14**, 1151–1158 (1997).
6. A. Lev and B. Sfez, "*In vivo* demonstration of ultrasound-modulated light technique," J. Opt. Soc. Am. A **20**, 2347–2354 (2003).
7. M. Gross, P. Goy, B. C. Forget, M. Atlan, F. Ramaz, A. C. Boccara, and A. K. Dunn, "Heterodyne detection of multiply scattered monochromatic light with a multipixel detector," Opt. Lett. **30**, 1357 (2005).
8. C. Ayata, A.K. Dunn,Y. Gursoy-Ozdemir,Z. Huang,D.A. Boas and M.A. Moskowitz, "Laser Speckle Flowmetry for the Study of Cerebrovascular Physiology in Normal and Ischemic Mouse Cortex," J. Cereb. Blood Flow Metab. **24**, 744-755 (2004).
9. M. Atlan, M. Gross, T. Vitalis, A. Rancillac, B. C. Forget, and A. K. Dunn, "Frequency-domain, wide-field laser doppler in vivo imaging," Opt. Lett. submitted 3/21/2006, accepted for publication (2006).
10. A. Lev, Z. Kotler, and B. Sfez, "Ultrasound tagged light imaging in turbid media in a reflectance geometry," Opt. Lett. **25**, 378 (2000).
11. A. L. an B. G. Sfez, "Direct, noninvasive detection of photon density in turbid media," Opt. Lett. **27**, 473 (2002).
12. M. Gross, P. Goy, and M. Al-Koussa, "Shot-noise detection of ultrasound-tagged photons in ultrasound-modulated optical imaging," Opt. Lett. **28**, 2482-2484 (2003).
13. M. Atlan, B.C. Forget, F. Ramaz, A.C. Boccara, and M. Gross, "Pulsed acousto-optic imaging in dynamic scattering media with heterodyne parallel speckle detection," Opt. Lett. **30**, 1360–1362 (2005).
14. G. Yao and L.V. Wang, "theoretical and experimental studies of ultrasound modulated optical tomography in biological tissues," Appl. Opt. **39**, 659 (2000).
15. S. Lévêque, A. C. Boccara, M. Lebec, and H. Saint-Jalmes, "Ultrasonic tagging of photon paths in scattering media: parallel speckle modulation processing," Opt. Lett. **24**, 181 (1999).
16. F. Ramaz, B. C. Forget, M. Atlan, A. C. Boccara, M. Gross, P. Delaye, and G. Roosen, "Photorefractive detection of tagged photons in ultrasound modulated optical tomography of thick biological tissues," Opt. Express **12**, 5469–5474 (2004).
17. T. W. Murray, L. Sui, G. Maguluri, R. A. Roy, A. Nieva, F. Blonigen, and C. A. DiMarzio, "Detection of ultrasound-modulated photons in diffuse media using the photorefractive effect," Opt. Lett. **29**, 2509 (2004).
18. E. Bossy, L. Sui, T. W. Murray, and R. A. Roy, "Fusion of conventional ultrasound imaging and acousto-optic sensing by use of a standard pulsed-ultrasound scanner," Opt. Lett. **30**, 744 (2005).
19. F. J. Blonigen, A. Nieva, C. DiMarzio, S. Manneville, L. Sui, G. Maguluri, T. W. Murray, and R. A. Roy, "Computations of the acoustically induced phase shifts of optical paths in acoustophotonic imaging with photorefractive-based detection," Appl. Opt. **44**, 3735 (2005).
20. L. Sui, R. A. Roy, C. DiMarzio, and T. W. Murray, "Imaging in diffuse media with pulsed-ultrasound-modulated light and the photorefractive effect," Appl. Opt. **44**, 4041 (2005).
21. M. Gross, F. Ramaz, B. C. Forget, M. Atlan, A. C. Boccara, P. Delaye, and G. Roosen, "Theoretical description of the photorefractive detection of the ultrasound modulated photons in scattering media," Opt. Express **13**, 7097–7112 (2005).
22. S. Bian, J. Frejlich, "Photorefractive response time measurement in GaAs crystals by phase modulation in two wave mixing," Opt. Lett. **19**, 1702-1704 (1994)
23. B. Sugg, K.V. Shcherbin, J. Frejlich, enquoteDetermination of the time constant of fast photorefarctive materials using the phase modulation technique, Appl. Phys. Lett. **66**, 3257-3259 (1995).
24. G. Brost, J. Norman, S. Odoulov, K. Shcherbin, A. Shumelyuk, and V. Tarano, "Gain Spectra of beam coupling in photorefractive semiconductors," J. Opt. Soc. Am. B, **15**, 2083-2091 (1998).
25. P. Delaye, S. de Rossi, G. Roosen, "High amplitude vibrations detection on rough surfaces using a photorefractive velocimeter," Opt. and Las. in Eng. **33** 335-347 (2000).
26. B. Campagne, A. Blouin, L. Pujol, J.P. Monchalin, "Compact and fast response ultrasonic detection device based on two-wave mixing in a gallium arsenide photorefractive crystal," Rev. Sc. Inst. **72** 5, 2478-2482 (2001).
27. P. Delaye, L. A. de Montmorillon, and G. Roosen, "Transmission of time modulated optical signals through an absorbing photorefractive crystal," Opt. Commun. **118**, 154 (1995).
28. P. Yeh, "Introduction to Photorefractive Nonlinear Optics" Wiley eds, ISBN: 0-471-58692-7.

1. Introduction

Optical imaging through many centimeters of biological tissues still remains a challenge, since the media are highly scattering. No conventional images can be performed. Diffuse Optical Tomography (DOT) is a pure optical methods which provides images following a reverse treat-

#75639 - $15.00 USD Received 2 October 2006; revised 17 November 2006; accepted 27 November 2006

ment of the local diffusion equation [1]. Since a *flux* is measured, it is not sensitive to *in vivo* motion, compared to interferometric techniques. But this numerical approach can be time consuming according to the enormous quantity of data that are involved, and up to now, accurate resolution approaches $1cm^3$.

Acousto-optic imaging (AOI) is an hybrid technique that uses the perturbation brought by ultrasound (US) inside a medium. This alternative tool provides direct *in-vivo* tomographies of objects (*e.g* tumors) embedded through thick biological tissues (some *cm*) [2–5]. In this approach, the acousto-optic signal gives an optical contrast located at the position of the ultrasound, with a resolution close to ultrasound imaging, *e.g.* $1mm^3$. In many experiments, one performs measurements on the so-called *tagged*-photons, which are the one shifted from the US frequency through their path within the ultrasonic volume. The quantity of these useful photons represents no more than 1% of the total amount of light detected through the sample, which still remains weak.

Since acousto-optic effect is a coherent process, it requires the use of a laser with a large coherence length, but, because of the multiple scattering of photons through the sample, the field detected at the output of the sample has a speckle nature. The signal is thus coherent in time, but not in space. In order to detect selectively the pertinent *tagged*-photons an adequate coherent detection has to be performed.

Another difficulty arises on living tissues. The different motions within tissues, like the blood circulation and/or the brownian motion, reduce the coherence time of the electric field **E**. Nevertheless, $\mathbf{E}(t)$ and $\mathbf{E}(t')$ remains correlated if $|t-t'| < \tau_c$ (where $\tau_c \sim 0.1ms$ is the field decorrelation time [6, 7]). Since the field **E** is detected by a coherent technique, the contrast of the signal thus depends on the measurement time, and goes down for longer time. There is thus no benefit to work with an acquisition time larger than τ_c. Although speckle decorrelation is usually considered as a source of noise in many situations, the variations of its contrast can be used to measure some velocities distributions, as it has been done at low depth penetrations on a rat brain [8, 9].

Many configurations have been explored in order to extract the signal blurred from this speckle pattern, whether using a set of optical fibers coupled to a single photo-detector [6, 10, 11], or an interferometric setup coupled to CCD cameras [12–14]. In the first case, one has to image onto the detector one (or a few) grains of speckle (to avoid to wash out the signal by averaging speckles with different phases). The detection can be very fast, thus not sensitive to decorrelation, but the amount of *flux* is weak, because the detector *etendue* (product of the area by solid angle) is low. In the second approach, the coherent detection is done on a multi pixel detector like a CCD camera [15]. The *etendue* is much larger ($\sim 10^6$ pixels), and it is possible, by using heterodyne holography detection, to perform selective shot noise limited detection of the *tagged*-photons [12]. Nevertheless, the detection is slower. The CCD detection cycling ratio is thus low, because the CCD exposure time (which must be about τ_c to keep a good contrast) is much shorter than the image grabbing time *i.e.* the time to transfer the image data to the computer ($100ms$ for 10^6 pixels and a grabbing frequency of 10^7 Hz).

More recently has appeared a new technique with a high *etendue* and a high velocity response [16, 17]. The setup consists in a Mach-Zehnder interferometer where the recombination plate is a photorefractive (PR) crystal. Its great advantage is to obtain from the reference beam onto the crystal a diffracted component in the *same* direction as the signal beam, and with the *same* speckle characteristics. Since those beams are wavefront-adapted, they interfere coherently and thus the CCD camera can be replaced with a large area single photodetector ($1cm^2$), much more rapid and with a reduced post-treatment, that gives the possibility to observe the signal in *real-time*. To our knowledge, two groups have recently published results on this new techniques [16–21]. Sui et *al.* [20], who uses a BSO single crystal in the green region, has demonstrated

#75639 - $15.00 USD Received 2 October 2006; revised 17 November 2006; accepted 27 November 2006

the possibility to measure the variation of the acousto-optic response along the US axis with application of pulsed ultrasound, while Gross et *al.* [21] and Ramaz et *al.* [16] have presented and modelized various configurations in a *cw* regime for the US, presenting results obtained with a single crystal of GaAs at a working wavelength of 1064*nm*.

The PR detection of the *tagged*-photons is expected to be fast and potentially able to yield a good contrast for *in vivo* images. In practical situation, the PR velocity is not limited by the photodetector (photodiode + electronic), but by the PR crystal response time τ_{PR}. To get an optimum detection in terms of *Signal to Noise* ratio (*e.g SNR*), τ_{PR} has to be adjusted to the experimental *in situ* conditions. From a practical point of view, a compromise requires $\tau_{PR} \simeq \tau_c$. This is explained as follows : in our case, the temporal variations encountered (ultrasound, *in vivo* motion) act on the *phase* of the speckle pattern. If τ_{PR} is large ($\tau_{PR} > \tau_c$), speckle decorrelates faster than the build-up of the photorefractive effect (phase hologram), the hologram washes out and the contrast of the signal goes down (phase averaging close to zero).
If τ_{PR} is short ($\tau_{PR} < \tau_c$), the speckle contrast is good because the phase hologram established within the PR crystal "follows" speckle decorrelation. But it also means that detection will have to detect signals over a larger bandwidth : this will bring additional noise, and thus will reduce *SNR*. Another difficulty arises with rapid τ_{PR} that are generally obtained with a high power of the reference beam. Since the *DC* component of the signal is mainly due to the scattering of the reference towards detection, it produces a dominant contribution within the noise spectrum. Finally, the frequency modulation of the ultrasound (*e.g* amplitude or phase) must be larger than $1/\tau_{PR}$. If not, the phase of the diffracted beam and the speckle output pattern are very close-related and thus the temporal contrast of the interference term between the signal and the reference beam is weak. As a conclusion, the performances of the *tagged*-photon PR detection setup are strongly dependent on the photorefractive crystal, thus it is necessary to measure τ_{PR} *in situ*, and compare it with τ_c. The response time τ_{PR} is founded to be 150*ms* for the BSO setup [20], and 5*ms* for GaAs one [21]. This quantity depends on the crystal, but also on the optical configuration of the setup (i.e. power and area of the PR pump beam).

The experimental evaluation of τ_{PR} can be performed through temporal or frequency measurements. In the first case, the build-up of the photorefractive grating is evaluated through time resolved measurements of the variation of the detected signal when one or several beams that create the grating are put onto the crystal. These methods are convenient for crystals with a slow response time. When fast response time has to be determined, the experimental set-up becomes generally more complex with the necessity to use high-speed optical shutters with a high optical contrast or to use pulsed lasers. Despite being very simple in its principle, temporal measurements can be difficult to implement experimentally. This problem is canceled in the frequency domain, where we measure the frequency response of the grating to a perturbation. This method to which belongs the experiments we present here, is the best suited for rapid crystals. Two standards configurations are generally used to implement the experiment. Either we use a phase (or less often an intensity) modulated beam in a two wave mixing set-up [22, 23] and we measure the amplitude of the detected signal as a function of the frequency (at one or several harmonics of the modulation), the cut-off frequency being related to the build-up time of the grating. The second alternative consists in using a moving grating [24] obtained by the interference between two beams with slightly different frequencies (or obtained through linearly phase modulating one of the beam). At high speed, the grating is erased and the measurement of the photorefractive gain as a function of this speed (or of the frequency difference) gives access to the response time of the photorefractive crystal. The technique we propose is related to the frequency measurement case. We use our experimental set-up for acousto-optical imaging to obtain a direct access to the response time of the photorefractive crystal in the exact condition of the measurement (grating spacing, pump beam power, nature of the crystal,...),

#75639 - $15.00 USD Received 2 October 2006; revised 17 November 2006; accepted 27 November 2006

without the use of an external experimental setup for additional measurements. The frequency de-tuning method that we will depict is not sensitive to the photodetection response, since the measurement is performed at a single frequency. We have made measurements of τ_{PR} as a function of the reference beam intensity for two types of GaAs crystals. The shortest τ_{PR} we have obtained ($0.25ms$) is compatible with the decorrelation time encountered in thick biological tissues ($\tau_c \sim 0.1ms$ [7]).

2. Presentation of the method

The analysis of the speckle pattern at the exit of the scattering medium under an ultrasonic excitation has been described in a previous paper [21]. When necessary, we will refer to the results and notations used in this reference. The application of a *cw* ultrasonic excitation (frequency ω_{US}) modulates the optical path along the volume of the US via the acousto-optic effect, thus the optical phase of light crossing the US volume is modulated at the ultrasonic frequency. This phase modulation effect classically generates sidebands on the laser spectrum (frequency ω_0). These additional frequencies ω_n are written generically as

$$\omega_n = \omega_0 \pm n\omega_{US} \tag{1}$$

The different components are spatially uncorrelated because of their speckle character [21]. Their weight depends mainly on the acoustic pressure delivered by piezo-transducer via a Bessel's function J_n, which is integrated over the path length of light within the ultrasonic volume, as mentioned in Eq. (12) of reference [21]. The field at frequency ω_0 corresponds to the so-called *diffused photons* through the sample, while fields at frequency $\omega_{\pm 1}$ corresponds to the *tagged* photons, which are in minority compared to the diffused photons (typically 1%). The addition of a slow phase or amplitude modulation (frequency ω_{mod}) on the US is quite heavy to develop analytically, but once again, it will generate sidebands. As a consequence, the speckle field contains many harmonics of generic expression:

$$\omega_{n,p} = \omega_0 \pm n\omega_{US} \pm p\omega_{mod} \tag{2}$$

The hologram built within the photorefractive crystal by the interference between the speckle field and the reference beam (plane wave, frequency ω that can be different from the laser frequency ω_0) contains *a priori* many frequencies of the form $(\omega_{n,p} - \omega)$, but only the slow varying components (i.e. $|\omega_{n,p} - \omega|\tau_{PR} < 1$) can contribute to the establishment of this hologram.

In the case of semiconductor crystals, where deep traps are responsible for the photorefractive effect, this time can be smaller than $100\mu s$ for a flux density of some $Watts/cm^2$ [25, 26]. In any case, it cannot follow an ultrasonic modulation ω_{US} at $2MHz$, as it is our case. As a consequence, the frequency difference between the reference beam and the signal beam must be reasonably close to an harmonic of the ultrasonic frequency ω_{US}. When no frequency difference exists, *e.g* for $n = 0$, the hologram corresponds to the speckle associated to the *diffused* photons. The hologram linked to the *tagged*-photons is obtained when the difference is ω_{US}, *e.g* for $n = 1$. Whatever the selected photons, the time evolution $f(t)$ of the interference illumination pattern is smoothed by the convolution of the photorefractive response of the crystal, and thus becomes the response of the hologram. The photorefractive response of the crystal can be in many cases approximated by a single exponential growth [27]:

$$G(z,t) = \gamma z \frac{e^{-t/\tau_{PR}}}{\tau_{PR}} \tag{3}$$

where z represents the main axis propagation inside the crystal while γ stands for the photorefractive gain. The build-up of the photorefractive effect has a characteristic rate (*e.g* $1/\tau_{PR}$)

#75639 - $15.00 USD Received 2 October 2006; revised 17 November 2006; accepted 27 November 2006

which depends on the intrinsic properties of the crystal, but also on the total *flux* density (W/cm^2) of the beams overlapping within the volume [28]. This means that the crystal plays the role of a low-pass filter in the frequency domain, with a cut-off frequency $\omega_c = 1/\tau_{PR}$. When the *flux* of the reference beam is weak, the response of the crystal is very slow compared to the modulation ω_{mod} : the hologram is mainly static, and thus proportional to the mean value of $f(t)$, e.g $< f(t) >$. This is the reason why under a low frequency phase modulation of the US $(1kHz)$, we initially applied a rectangular shape $[0,\pi]$ with a non zero mean value (a cyclic ratio $x \simeq 0.25$ has been chosen to optimize a lock-in detection) [16]. The situation is slightly different if one deals with *in vivo* imaging, because ω_c and ω_{mod} will have the same magnitude: though filtered, the hologram can now follow this frequency. We will see now how to use this property to measure τ_{PR} *in situ* in the case of $n = 0$.

3. Frequency shift dependence of the acousto-optic response

Let us consider for a sake of clarity a *single path i* within the medium traveled by the n^{th} component of the acousto-optic field (main frequency $\omega_n = \omega_0 + n\omega_{US}$). Since the fields associated to the different pathes are random in phase, the contribution on the surface of the detector of their interference with the diffracted reference will add incoherently. Thus, conclusions drawn on the time evolution of the signal related to a *single path* will remain the same for the entire signal.

Let us consider the field diffused along the path i as a scalar quantity $E_{S,i}(\mathbf{r},t)$ since we will use in the following a linearly polarized beam $\mathbf{E}_R(\mathbf{r},t)$ as reference. The former can be developed into harmonic components n as following :

$$E_{S,i}(\mathbf{r},t) = \sum_n E_{S,i}^{\omega_n}(\mathbf{r},t) \tag{4}$$

If we decompose the travel path length s_i into a static broad distribution $(s_{i0} >> \lambda)$ and a time varying contribution $\delta s_i(t)$, we can write the field component $E_{S,i}^{\omega_n}$ according to Eq. (12) of [21]:

$$E_{S,i}^{\omega_n}(\mathbf{r},\, t) = a_i(\mathbf{r})\;\; e^{-j\theta_i(\mathbf{r})} J_n(\beta_i(t))\; e^{j\omega_0 t}\; e^{jn\omega_{US}t}\; e^{jn(\phi_i(t)+\pi/2)} \tag{5}$$

where $\beta_i(t) = 2\pi/\lambda|\delta s_i(t)|$ and $\phi_i(t) = arg(\delta s_i(t))$ depend on the acoustic pressure in case of an ultrasonic excitation, while $a_i(\mathbf{r})$ characterizes the optical contrast, and $\theta_i(\mathbf{r}) = 2\pi/\lambda s_{i0}(\mathbf{r})$ is random and evenly distributed over $[0..2\pi]$. To detect $E_{S,i}^{\omega_n}$, the frequency of the plane wave reference beam (or PR pump beam) must be close to ω_n. In presence of a frequency shift $\Delta\omega$ the pump beam can be written as:

$$E_R(\mathbf{r},t) = E_0 e^{j(\omega_0 + n\omega_{US})t} e^{j\Delta\omega t} \tag{6}$$

The time varying photorefractive index $\Delta n(\mathbf{r},t)$ (hologram) inside the PR crystal is proportional to the modulation depth of the interference pattern convoluted by the temporal response of the crystal. We have thus:

$$\Delta n(\mathbf{r},t) = \left(\frac{E_{S,i}^{\omega_n}(\mathbf{r},t) E_R^*(\mathbf{r},t)}{E_{S,i}^{\omega_n}(\mathbf{r},t) E_{S,i}^{*\omega_n}(\mathbf{r},t) + E_R(\mathbf{r},t) E_R^*(\mathbf{r},t)} \right) * G(z,t) \tag{7}$$

where "$*$" denotes a convolution product with respect to time t. When the reference is much larger than the signal beam, the previous expression can be simplified into :

$$\Delta n(\mathbf{r},t) \simeq \eta \frac{a_i(\mathbf{r})\; e^{-j\theta_i(\mathbf{r})}}{E_0} \left(J_n(\beta_i(t))\; e^{jn(\phi_i(t)+\pi/2)}\; e^{-j\Delta\omega t} \right) * \left(\frac{e^{-t/\tau_{PR}}}{\tau_{PR}} \right) \tag{8}$$

#75639 - $15.00 USD Received 2 October 2006; revised 17 November 2006; accepted 27 November 2006

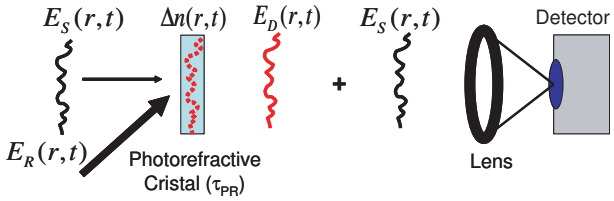

Fig. 1. Spatio-temporal principle for a self-adaptive wavefront holography using a photorefractive crystal with time constant τ_{PR}. As mentionned in section 3, the interference pattern between the signal $E_S(r,t)$ and the reference $E_R(r,t)$ beam is recorded within the crystal via its refractive index $\Delta n(r,t)$: the reference beam diffracts a spatial replica of the signal $E_D(r,t)$, smoothed in time by the finite photorefractive time establishment.

where $\eta = \gamma z$ stands for the diffraction efficiency of the photorefractive effect. As seen above, the photorefractive response of the crystal is characteristic of a low-pass frequency filter: the response of the system to a monochromatic excitation is linear, but it can be damped and phase-shifted if the frequency is close or superior to the *cut-off* frequency of the filter. In the particular case here of Eq. (8), the refractive index exhibits a shift in frequency of $-\Delta\omega$. The pump beam (frequency $\omega_n + \Delta\omega$) diffracted by the PR hologram yields a diffracted beam $E_{D,i}(\mathbf{r},t) = \Delta n(\mathbf{r},t) E_R(\mathbf{r},t)$; its main frequency is consequently the same as the signal beam *e.g* ω_n and thus *independent* of $\Delta\omega$ since we can write :

$$E_{D,i,\Delta\omega}^{\omega_n}(\mathbf{r},t) = \eta a_i(\mathbf{r})\, e^{-j\theta_i(\mathbf{r})} \left[\left(J_n(\beta_i(t))\, e^{jn(\phi_i(t)+\pi/2)}\, e^{-j\Delta\omega t} \right) * \left(\frac{e^{-t/\tau_{PR}}}{\tau_{PR}} \right) \right] e^{j(\omega_0 + n\omega_{US})t} e^{j\Delta\omega t} \tag{9}$$

Though out of the scope the paper, the development of Eq. (9) in the general case shows that $E_{D,i,\Delta\omega}^{\omega_n}$ evolves at ω_n and that its magnitude and phase depend on $\Delta\omega$. This last remark is important and shows that it is possible to measure the acousto-optic signal as a function of $\Delta\omega$ in using for example a detection at a single frequency (*e.g* with a lock-in detection). Moreover, the $\Delta\omega$ spectrum that can be obtained is not sensitive to the finite frequency response of the detection chain.

This last expression also demonstrates the major topic of the technique : the spatial variations (amplitude and phase) of components $E_{D,i,\Delta\omega}^{\omega_n}(\mathbf{r},t)$ and $E_{S,i}^{\omega_n}(\mathbf{r},t)$ are *coherent*. As a generalization, the speckle field at the output of the sample (*e.g* summation over i) builds a wavefront adapted reference that can interfere *coherently* onto a *single detector* [21], thus providing a simple solution to measure *in real time* the acousto-optic signal.

We will consider now that the ultrasonic excitation is periodically modulated at frequency ω_{mod}. This modulation is either a pure phase modulation (PM) or pure amplitude modulation (AM) with a modulation factor $H(t)$. According to Eq. (35) of [21], $\beta_i(t)$ and $\phi_i(t)$ become :

$$\beta_i(t) = H_{AM}(t)\beta_i \tag{10}$$

or

$$\phi_i(t) = \phi_i + H_{PM}(t) \tag{11}$$

To develop in a generic way $E_{S,i}^{\omega_n}(\mathbf{r},t)$, let us introduce the Fourier's expansion of $J_n(\beta_i)\, e^{-jn\phi_i}$ (*i.e.* the expansion of $H_{AM}(t)$ or $H_{PM}(t)$) as follows:

$$e^{-jn\phi_i(t)} J_n(\beta_i(t)) \equiv \sum_p c_{i,n,p}\; e^{jp\omega_{mod}t} \tag{12}$$

#75639 - $15.00 USD Received 2 October 2006; revised 17 November 2006; accepted 27 November 2006

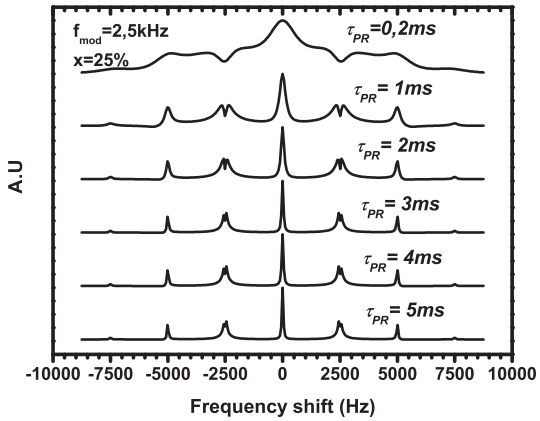

Fig. 2. Simulation of the response $S^{\Delta\omega}_{\omega_{mod}}$ for different τ_{PR}, with a rectangular $[0,\pi]$ phase modulation of the US excitation and a cyclic ratio of 25%

One get then from Eq. (5):

$$E^{\omega_{n,p}}_{S,i}(\mathbf{r},t) = a_i(\mathbf{r})\, e^{-j\theta_i(\mathbf{r})}\, e^{jn(\phi_i+\pi/2)}\, e^{j\omega_0 t}\, e^{jn\omega_{US}t} \sum_p c_{i,n,p}\, e^{jp\omega_{mod}t} \tag{13}$$

where i, n and p are, as mentioned above, the travel pass index, the US frequency (ω_{US}) harmonic index and the modulation frequency (ω_{mod}) harmonic index respectively. Taking into account the convolution product within Eq. (8), we can write the diffracted signal (Eq.(9)) as follows:

$$E^{\omega_{n,p}}_{D,i,\Delta\omega}(\mathbf{r},t) = \eta\; a_i(\mathbf{r})\, e^{-j\theta_i(\mathbf{r})}\, e^{jn(\phi_i+\pi/2)}\, e^{j\omega_0 t}\, e^{jn\omega_{US}t} \sum_p \frac{c_{i,n,p}(\mathbf{r})}{1+j(p\omega_{mod}-\Delta\omega)\tau_{PR}}\, e^{jp\omega_{mod}t} \tag{14}$$

This last expression exhibits more specifically how each frequency component of $\Delta n(\mathbf{r},t)$, *e.g* $(p\omega_{mod}-\Delta\omega)$ is smoothed and phase shifted by the low-pass filter associated to the photorefractive effect inside the crystal (see Eq. (3)). The AO signal $S^{\Delta\omega}_{i,n}(t)$ measured by the photodetector results from the interferences between the E_S and E_D fields. We get:

$$S^{\Delta\omega}_{i,n}(t) = \mathbf{Re}\left[2E^{*\omega_n}_{S,i}(\mathbf{r},t)\;\; E^{\omega_n}_{D,i,\Delta\omega}(\mathbf{r},t)\right] = 2\eta a_i^2(\mathbf{r})\;\mathbf{Re}\left[\sum_{k,p}\frac{c^*_{i,n,k}\, c_{i,n,p}\, e^{j(p-k)\omega_{mod}t}}{1+j(p\omega_{mod}-\Delta\omega)\tau_{PR}}\right] \tag{15}$$

where **Re** is the real part operator. This last expression shows a dependency of the signal with τ_{PR} but also with the frequency de-tuning $\Delta\omega$ of the reference. In addition, resonances will occur when the de-tuning matches an harmonic of the modulation, *e.g* $\Delta\omega \equiv p\omega_{mod}$.

As an example, we have considered a pure rectangular phase modulation of the US with a 25% cyclic ratio and a lock-in detection at ω_{mod}, what fixes the coefficient $c_{i,n,k}$. In Eq. (15), the $k-p=\pm 1$ terms are thus only considered. We have calculated the signal for the US harmonic component $n=1$ for different values of τ_{PR} as a function of $\Delta\omega$. The $\Delta\omega$ spectra are shown on Fig. 2. As seen, the shapes of the spectra are quite complicated and the extraction of τ_{PR} from the measurement of $S^{\Delta\omega}_{i,n}(t)$ is *a priori* not straightforward.

#75639 - $15.00 USD Received 2 October 2006; revised 17 November 2006; accepted 27 November 2006

4. Lock-in detection of the signal with an amplitude modulated ultrasonic excitation

Let us consider at present a rectangular (AM) ultrasonic excitation the US at frequency ω_{mod} with a cyclic ratio x:

$$H_{AM}(t) = \text{Rect}\left(\frac{t}{xT}\right) * \sum_m \delta(t - mT) \tag{16}$$

where Rect and δ are the rectangle and Dirac functions and $T = 2\pi/\omega_{mod}$ the modulation period. We will consider the field associated to the diffused photons, *e.g* $n = 0$. Eq. (12) becomes:

$$J_0\left(\beta_i H_{AM}(t)\right) \equiv \sum_p c_{i,0,p}\ e^{jp\omega_{mod}t} = 1 + (J_0(\beta_i) - 1) \sum_p x\,\text{sinc}(p\pi x)\, e^{-jp\pi x}\, e^{jp\omega_{mod}t} \tag{17}$$

so we get the expansion coefficients $c_{i,0,p}$ that are needed to calculate $S_{i,0}^{\Delta\omega}(t)$ with Eq. (15):

$$c_{i,0,0} = (1-x) + x\, J_0(\beta_i) \tag{18}$$

$$c_{i,0,p\neq 0} = x\,(J_0(\beta_i) - 1)\,\text{sinc}(p\pi x)\, e^{-jp\pi x} \tag{19}$$

We will consider a lock-in detection operating at ω_{mod} so that $k - p = \pm 1$, and a symmetric rectangular shape modulation $H_{AM}(t)$, *e.g* for $x = 1/2$. The coefficients $c_{i,0,k}$ vanish for $k = \pm 2, \pm 4...$ (because $\text{sinc}(k\pi/2)$ is zero). In Eq. (15), the only terms that contribute to the signal are thus $k = 0, p = \pm 1$ and $p = 0, k = \pm 1$as all other harmonics are even and thus verifies $k - p \geq 2$. The lock-in detection used with a symmetric $[0,1]$ rectangular-shape reference measures the P and Q quadrature components of the signal as follows :

$$P(\Delta\omega) = \int S_{i,0}^{\Delta\omega}(t)\ \cos(\omega_{mod}t - \pi/2)\, dt \tag{20}$$

$$Q(\Delta\omega) = \int S_{i,0}^{\Delta\omega}(t)\ \sin(\omega_{mod}t - \pi/2)\, dt \tag{21}$$

The development of $P(\Delta\omega)$ component exhibits three contributions $P(\Delta\omega) = P_0 + P_+ + P_-$ while $Q(\Delta\omega)$ contains two terms $Q(\Delta\omega) = Q_+ + Q_-$, as defined below :

$$P_0(\Delta\omega) = \frac{2A_{i,0}}{1 + (\Delta\omega\tau_{PR})^2} \tag{22}$$

$$P_\pm(\Delta\omega) = \frac{A_{i,0}}{1 + (\omega_{mod} \mp \Delta\omega)^2\ \tau_{PR}^2} \tag{23}$$

$$Q_\pm(\Delta\omega) = -\frac{A_{i,0}}{1 + (\omega_{mod} \mp \Delta\omega)^2\ \tau_{PR}^2}(\omega_{mod} \mp \Delta\omega)\tau_{PR} \tag{24}$$

where

$$A_{i,0} = \frac{1}{\pi}\eta\ a_i^2(\mathbf{r})\left[1 + \frac{1}{2}\left(J_0(\beta_i) - 1\right)\right]\ \left[J_0(\beta_i) - 1\right] \tag{25}$$

The lock-in signals can also been expressed by a magnitude R and a phase φ (with $P \equiv R\sin\varphi$ and $Q \equiv R\cos\varphi$) that is written in our case :

$$R(\Delta\omega) = \sqrt{P^2(\Delta\omega) + Q^2(\Delta\omega)} \tag{26}$$

$$tan\varphi(\Delta\omega) = \frac{P(\Delta\omega)}{Q(\Delta\omega)} \tag{27}$$

#75639 - $15.00 USD Received 2 October 2006; revised 17 November 2006; accepted 27 November 2006

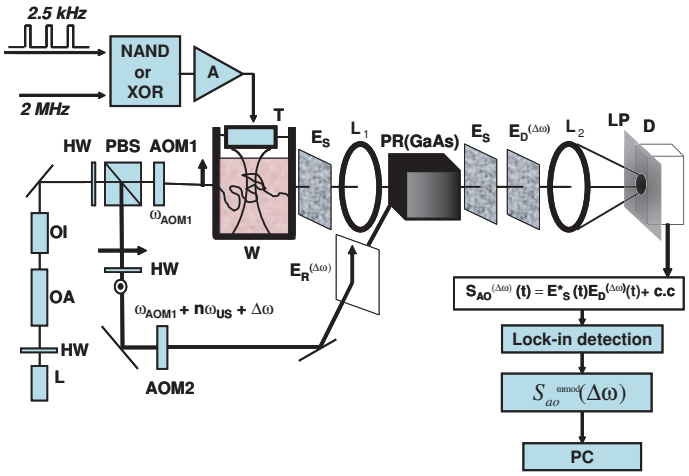

Fig. 3. Experimental setup : (L) 1*W* Nd:YAG laser, (OA) 5*W* Yb-doped optical amplifier, (OI) optical Faraday isolator, (HW) half-wave plate, (AMO1,2) acousto-optic modualtor, (W) water tank, (PBS) polarizing beam-splitter, (T) acoustic-transducer, (PR) photorefractive GaAs crystal, (LP) linear polarizer, (L1,2) wide aperture collection lenses, (D) $\phi = 5mm$ InGaAs photodiode.

If the modulation frequency ω_{mod} is high enough compared with $1/\tau_{PR}$, $R(\Delta\omega)$ exhibits three well separated resonances ($\Delta\omega = 0, \pm\omega_{mod}$) that allow an easy measurement of τ_{PR}. The central line ($\Delta\omega \simeq 0$) is related to $P_0(\Delta\omega)$. It has a lorentzian shape with a $FWHM = 2/\tau_{PR}$. The sidebands ($\Delta\omega \simeq \pm\omega_{mod}$) are related to $\sqrt{P_\pm^2(\Delta\omega) + Q_\pm^2(\Delta\omega)}$. They are square root lorentzian, with $FWHM = 2\sqrt{3}/\tau_{PR}$.
The slope measurement of $tan\varphi(\Delta\omega)$ near a sideband is also a possible way to determine τ_{PR} since we have according to Eq. (23) and Eq. (24):

$$tan\varphi_\pm(\Delta\omega \simeq \pm\omega_{mod}) \simeq \frac{P_\pm(\Delta\omega)}{Q_\pm(\Delta\omega)} \simeq -(\omega_{mod} \mp \Delta\omega)\tau_{PR} \tag{28}$$

5. Experimental and results

The experimental configuration of the setup has been described in details elsewhere [16, 21] but let us recall the main features. We have built a Mach-Zehnder interferometer, where the recombination plate is a massive GaAs photorefractive crystal. The source (L) is a single mode frequency 1*Watt* Nd:YAG laser working at 1064*nm* (CrystaLaser corp.). Part of this laser $(150mW)$ can be injected into an ytterbium-doped fiber (OA) amplifier (Keopsys corp.) to produce a 5*Watt* source, still working at a single mode frequency. The addition of this element gives the opportunity to enlarge the power on the reference beam in order to reduce τ_{PR}. This will allow an ultrasonic modulation at higher frequency and thus use ultrasound in a pulsed regime.

We have chosen a 10*cm* thick solution of 20% intralipid to produce a scattering medium with no decorrelation. Two types of crystals have been considered, both oriented for a specific energy transfer configuration. Theses crystals come from the same ingot and we have measured an absorption coefficient $\alpha = 1.5cm^{-1}@1064nm$. The first type has (110), $(1-10)$ and (001) faces. The signal and the reference beams enter the (110) face (size $1.4 \times 2cm^2$) and propagate along the $< 001 >$ direction (thickness 1.4*cm*). In the second type crystal, the signal

#75639 - $15.00 USD Received 2 October 2006; revised 17 November 2006; accepted 27 November 2006

and the reference beams enter onto orthogonal faces, respectively $(11\sqrt{2})$ and $(11-\sqrt{2})$ (size $1.4\times 1.6cm^2$), in order to have a grating vector along the $<001>$ direction. Both signal and reference beam propagate through a thickness of $1.6cm$ within the crystal. In both crystal, the associated effective electro-optic coefficient is $|r_{eff}| = r_{41}$ and from a practical point of view, they exhibit approximately the same energy transfer efficiency (*e.g* $\eta = 25-35\%$). However, for semiconductors crystals, the response time τ_{PR} is known to be shorter for small angles between the beams (*i.e* for a small grating vector $\mathbf{K}_g$) and thus a co-directional configuration should respond faster that an orthogonal one [28]. Nevertheless, with a high enough reference intensity, the second type configuration could still be attractive because the reference inputs on a face orthogonal to the signal propagation, and thus it should produce less scattered light onto the InGaAs photo-detector (D) $(\phi = 5mm)$. A linear infrared gelatin polarizer (LP) has been positioned in front of the photo-detector, its axis being aligned along the reference beam polarization, which is vertical in our case. Since light at the output of the sample is completely depolarized by the scattering medium, it will suppress the field of orthogonal polarization (diffused and tagged), that do not participate to the interference signal, and thus enhance the signal-to-noise ratio (*SNR*). The excitation of the acoustic source is at a frequency of $2MHz$, and we add a phase or an amplitude modulation at $\omega_{mod} \simeq 2.5kHz$ in order to have a reasonable separation between the three resonances of $R(\Delta\omega)$. Finally, measurement of the signal is performed with a lockin detection using an $EG\&G$ 7260 model. We have put on each arm of the interferometer an acousto-optic modulator, that typically shifts the laser frequency of $78MHz$, and we add a low frequency shift $\Delta\omega$ on the reference in order to perform our measurements. When diffused photons are selected, each beam is shifted from $78MHz$, but if tagged-photons are selected, the reference beam is shifted from $80MHz$, while the signal is shifted from $78MHz$.

Figure 4 shows for R(4.a,4.b), φ(4.c,4.d), P(4.e,4.f), Q(4.g,4.h), the acousto-optical response with a lock-in detection at $2.5kHz$ as a function of $\Delta\omega$ taken with the static scattering medium of $10cm$ thick and comparable *flux* (e.g $300mW/cm^2$). As it is shown on the figures, fits can easily be performed on these spectra using the expression of P, Q, R depicted above, meaning that the simplified model of a single exponential growth remains valid here, even though we use a thick, and thus, absorbing sample [27]. The data (P,Q) shown on Fig. 4 represent each an acquisition time close to an hour; this explains the weak deviation between theory and experiment encountered for $R(4.b)$, $P(4.f)$, and $Q(4.h)$, due to a plausible drift of the various experimental parameters (laser source). This long acquisition time has been chosen here to collect a great number of data in order to validate the method and the analytical development. This time can significantly be reduced from a practical point of view, firstly because it is not necessary to performe these measurements for each position of the US. Secondly, a scan close to the resonance peaks, with a reduced time constant of the detection is still possible, since there is no need to measure τ_{PR} with a high accuracy. The fit of φ deviates significantly from theory outside resonances : this comes from the ratio nature of φ, that diverges when quantities become close to zero. We deduce from fit $\tau_{PR} = 0.5ms$ for the co-directional case, while we find $\tau_{PR} = 2.2ms$ in the orthogonal configuration. As expected, the first configuration is faster, but we have not already checked which solution could provide the best *SNR* in order to perform *in vivo* measurements. We have observed in some situations that the resonance shapes could deviate from theory, in the way that peaks can become sharper than expected. Such a point has already been reported by Brost et al [24] and occurs when the intensity profile of the beams (in particular the reference beam) is not uniform : in this case, one has to deal with a local intensity within the crystal, that induces a local τ_{PR}. Experimental shapes can still be fitted in considering τ_{PR} as a distribution within the crystal instead of a single value. But still, when the beam section is close to the input face of the crystal, this deviation is not significative, as shown in Fig. 4. The plots in Fig. 5 show the linear evolution of $1/\tau_{PR}$ as a function of the *flux* density of

#75639 - $15.00 USD Received 2 October 2006; revised 17 November 2006; accepted 27 November 2006

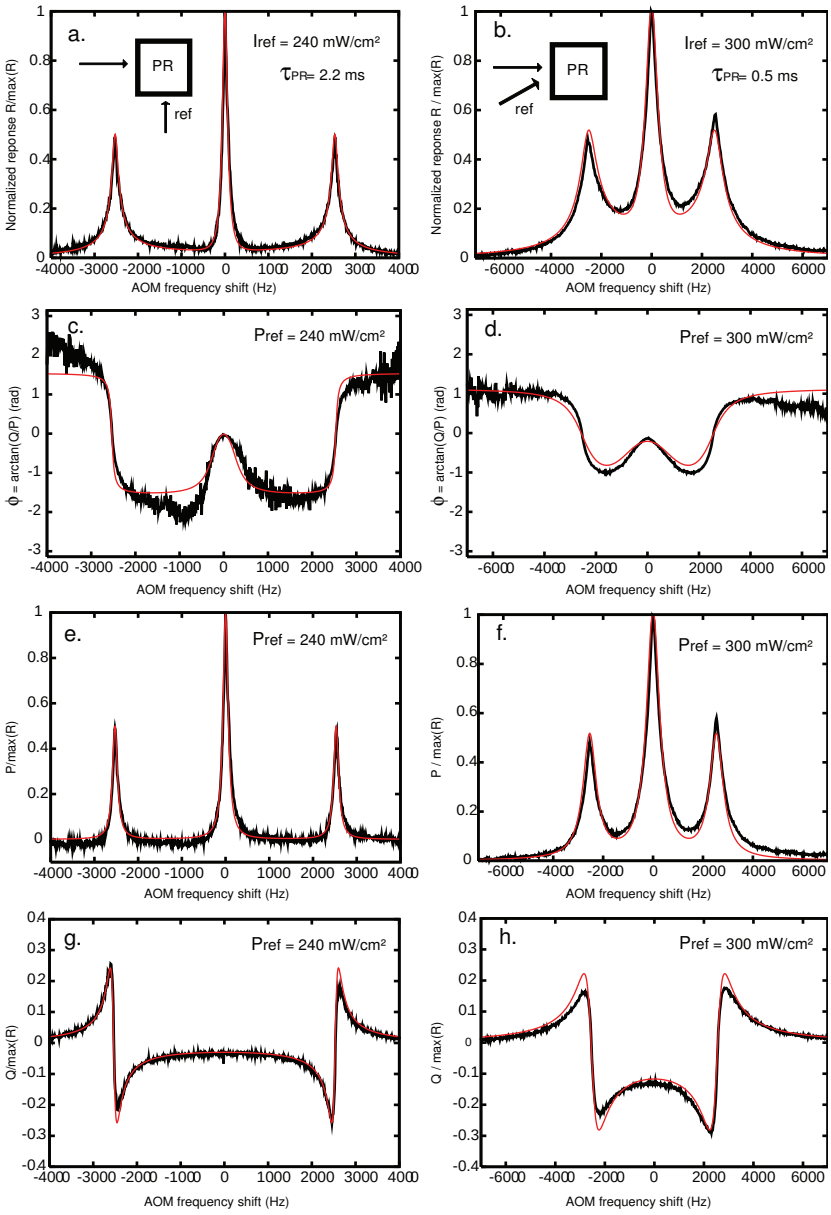

Fig. 4. Example of a lock-in measurement at $2.5kHz$ of the acousto-optic normalized response for a diluted scattering liquid as a function of a frequency shift $\Delta\omega/2\pi$ of the reference beam. The left column represents spectra (a,c,e,g) that have been obtained for an orthogonal pumping configuration with an incident *flux* of $240mW/cm^2$, while the right column (b,d,f,h) corresponds to a co-directional pumping with an incident *flux* of $300mW/cm^2$. From top to bottom, each line corresponds respectively to $R(\Delta\omega)$, $\varphi(\Delta\omega)$, $P(\Delta\omega)$, $Q(\Delta\omega)$ quantities, as defined in section 4. The width of the resonance peaks is connected to $1/\tau_{PR}$. Experimental data are black and theoretical fit prediction with a single parameter τ_{PR} is red (see text for details).

#75639 - $15.00 USD Received 2 October 2006; revised 17 November 2006; accepted 27 November 2006

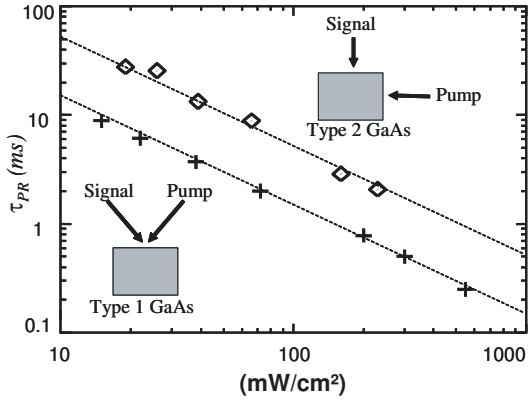

Fig. 5. Plot of the photorefractive response time τ_{PR} as a function of the incident intensity for a co-directional (type I crystal) or an orthogonal pumping configuration (type II crystal).

the reference beam, consistent with the standard Kukhtarev's model for photorefractivity [28]. The smallest value of $\tau_{PR} = 0.25ms$ has been obtained in the co-directional configuration with a pump beam of $560mW/cm^2$. According to Fig. 5, an extrapolation of the orthogonal-pumping measurements to this value should give a τ_{PR} of about 1 ms.

6. Conclusion

The speckle decorrelation time in living tissues affects the contrast when coherent optical measurements are performed. We have built an holographic setup that adapts the reference beam to the speckle output of the sample using a GaAs photorefractive crystal working in an energy transfer configuration with co-directional or orthogonal pumping. We have developed an original method that measures *in situ* the photorefractive response time of the crystal, that depends on the total *flux* density within the crystal volume. It is based on a lock-in detection with a symmetric amplitude excitation of the ultrasound plus a frequency detuning of the reference beam performed with acousto-optic modulators. This method is not sensitive to the frequency response of the detection. We are able at present to have a response time as short as $0.25ms$ with an intensity of the reference of $560mW/cm^2$, which will be compatible with fluctuations encountered during future *in vivo* imaging. A systematic study of the *SNR* as a function of the different parameters of the experiment (*e.g* τ_{PR}, τ_c, ω_{mod}) needs to be performed in order to optimize the quality of future acousto-optic tomographies.

Acknowledgements

This work is currently supported by a grant from the project *Cancéropôle Ile-de-France*.

#75639 - $15.00 USD Received 2 October 2006; revised 17 November 2006; accepted 27 November 2006